BIOCHEMISTRY
including biophysical chemistry & molecular biology

Article

pubs.acs.org/biochemistry

Kinetic Mechanism of DNA Polymerization Catalyzed by Human DNA Polymerase ε

Walter J. Zahurancik,[†,‡] Seth J. Klein,[§] and Zucai Suo*[,†,‡]

[†]Department of Chemistry and Biochemistry, [‡]The Ohio State Biochemistry Program, and [§]Department of Molecular Genetics, The Ohio State University, Columbus, Ohio 43210, United States

ABSTRACT: Eukaryotes require highly accurate and processive DNA polymerases to ensure faithful and efficient replication of their genomes. DNA polymerase ε (Polε) has been shown to catalyze leading-strand DNA synthesis during replication *in vivo*, but little is known about the kinetic mechanism of polymerization catalyzed by this replicative enzyme. To elucidate this mechanism, we have generated a truncated, exonuclease-deficient mutant of the catalytic subunit of human Polε (Polε exo-) and carried out pre-steady-state kinetic analysis of this enzyme. Our results show that Polε exo-, as other DNA polymerases, follows an induced-fit mechanism when catalyzing correct nucleotide incorporation. Polε exo- binds DNA with a K_d^{DNA} of 79 nM and dissociates from the E·DNA binary complex with a rate constant of 0.021 s^{-1}. Although Polε exo- binds a correct incoming nucleotide weakly with a K_d^{dTTP} of 31 μM, it catalyzes correct nucleotide incorporation at a fast rate constant of 248 s^{-1} at 20 °C. Both a large reaction amplitude difference (42%) between pulse-chase and pulse-quench assays and a small elemental effect (0.9) for correct dTTP incorporation suggest that a slow conformational change preceding the chemistry step limits the rate of correct nucleotide incorporation. In addition, our kinetic analysis shows that Polε exo- exhibits low processivity during polymerization. To catalyze leading-strand synthesis *in vivo*, Polε likely interacts with its three smaller subunits and additional replication factors in order to assemble a replication complex and significantly enhance its polymerization processivity.

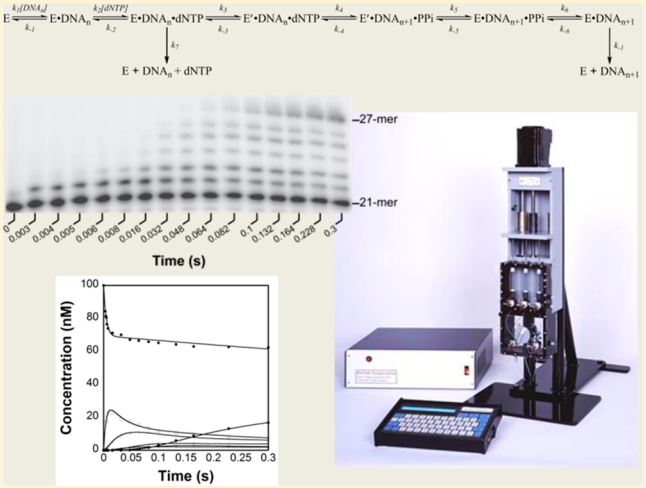

Three DNA polymerases (Pols), α, δ, and ε, efficiently and accurately replicate the majority of eukaryotic genomes.[1] Specifically, the Polα−primase complex primes the leading- and lagging-strand synthesis during DNA replication.[2] Studies involving mutagenic derivatives of Polε and Polδ have demonstrated that Polε is primarily responsible for leading-strand synthesis while Polδ plays a major role in lagging-strand replication.[2−4]

The Polε holoenzyme is a heterotetramer comprised of a single catalytic subunit (p261) and three smaller subunits (p59, p12, and p17). The N-terminal half of p261 contains the catalytic domain, while mapping studies have shown that the C-terminal half is necessary for interaction with the three smaller subunits.[5] Furthermore, *in vitro* DNA replication assays have shown that the catalytic domain fragment of p261 is as active as the Polε holoenzyme.[5] As with most replicative DNA polymerases, Polε possesses both DNA polymerase and 3′→5′ exonuclease proofreading activities, with the latter increasing the accuracy of DNA replication beyond the intrinsic fidelity of the former.[6] Among six families (A, B, C, D, X, and Y) of DNA polymerases, Polε belongs to the B-family. Because of a combination of high intrinsic fidelity and 3′→5′ proofreading activity, most B-family replicative DNA polymerases have fidelities in the range of 10^{-6}−10^{-8}, or one error per 10^6−10^8 nucleotide incorporations.[7] In addition to synthesizing the leading-strand during genomic replication, Polε is also involved in long-patch base excision repair *in vivo*.[8]

The kinetic mechanism of DNA polymerization catalyzed by the B-family replicative DNA polymerases such as bacteriophage T4 DNA polymerase[9] and *Sulfolobus solfataricus* PolB1[10] have been characterized by extensive pre-steady-state kinetic analysis. These polymerases catalyze nucleotide incorporation via an induced-fit mechanism which is outlined in Scheme 1. Within this mechanism, the polymerase first binds DNA and then an incoming nucleotide to form the ground-state ternary complex (E·DNA·dNTP). Next, the enzyme undergoes a conformational change (E′·DNA·dNTP) prior to phosphodiester bond formation and product releasing steps.

Recently, pre-steady-state kinetics has been applied to investigate correct and incorrect nucleotide incorporation catalyzed by yeast Polδ.[11] However, the mechanism of nucleotide incorporation catalyzed by either Polδ or Polε of

Received: June 21, 2013
Revised: August 15, 2013
Published: September 10, 2013

dx.doi.org/10.1021/bi400803v | *Biochemistry* 2013, 52, 7041−7049

Scheme 1. Minimal Kinetic Mechanism of DNA Polymerization Catalyzed by Human DNA Polymerase ε

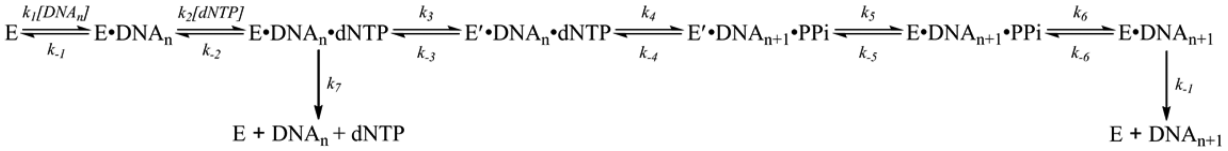

humans has not yet been established. Here, we report a minimal kinetic mechanism for correct nucleotide incorporation catalyzed by human Polε.

EXPERIMENTAL PROCEDURES

Materials. These chemicals were purchased from the following companies: [α-^{32}P]dTTP and [γ-^{32}P]ATP from PerkinElmer Life Sciences (Boston, MA), dNTPs from Bioline (Taunton, MA), S_p-dTTPαS and S_p-dATPαS from Biolog-Life Science Institute (Bremen, Germany). The DNA substrate (D-1) in Figure 1A was prepared as previously described.[12]

Expression and Purification of Human Polε. An orf encoding residues 1−1189 of the p261 subunit of human Polε was inserted into a modified pGEX4T3 vector C-terminal to a GST tag and a TEV cleavage site to generate vector pGEX4T3(TEV)/Polε(1−1189)-His$_6$. To generate an exonuclease-deficient mutant, two rounds of site-directed mutagenesis were used to make three amino acid substitutions (D275A/E277A/D368A). The TEV protease expression vector pRK603 was described previously.[13] Vectors pGEX4T3(TEV)/Polε exo-(1−1189)-His$_6$ and pRK603 were cotransformed into *Escherichia coli* expression strain BL21(DE3) Rosetta cells. The LB cultures were grown in the presence of 25 μg/mL kanamycin and 50 μg/mL carbenecillin at 37 °C until the OD_{600} of the cells reached 0.6. The protein expression was then induced with 70 μM IPTG. The cells were harvested and lysed by French press. The cell lysate was then clarified by ultracentrifugation (160000*g* at 4 °C for 40 min). Polε exo- was isolated from the cleared lysate by nickel ion affinity chromatography, followed by a MonoQ anion-exchange column, and finally by a Sephacryl S-200 HR size-exclusion column. Polε exo- was determined to be ∼95% homogeneous by SDS-PAGE analysis. The concentration of purified Polε exo- was measured by UV spectrometry at 280 nm using a calculated extinction coefficient of 156 760 M^{-1} cm^{-1}.

Pre-Steady-State Kinetic Assays. All assays using Polε exo- were performed at 20 °C using reaction buffer E (50 mM Tris-OAc, pH 7.4 at 20 °C, 8 mM $Mg(OAc)_2$, 1 mM DTT, 10% glycerol, 0.1 mg/mL BSA, and 0.1 mM EDTA). Fast reactions were carried out using a rapid chemical quench flow apparatus (KinTek). Notably, to prevent any residual cleavage of DNA by Polε exo-, Polε exo- was preincubated with DNA in the absence of Mg^{2+}, the catalytic metal ion.[14] All reported concentrations are final.

Measurement of the Rate Constant of DNA Dissociation from the Binary Complex. A preincubated solution of Polε exo- (50 nM) and 5′-radiolabeled D-1 (100 nM) was mixed with an unlabeled D-1 trap (2.5 μM) for 10 s to 20 min. After the mixing period, dTTP (133 μM) was added to the reaction mixture to initiate nucleotide incorporation. The reaction mixture was then allowed to incubate for an additional 15 s prior to be quenched by 0.37 M EDTA. Products were analyzed by sequencing gel analysis. The product concentrations were plotted against mixing times, and the data were fit to the following equation: [product] = $A \exp(-kt) + C$, where

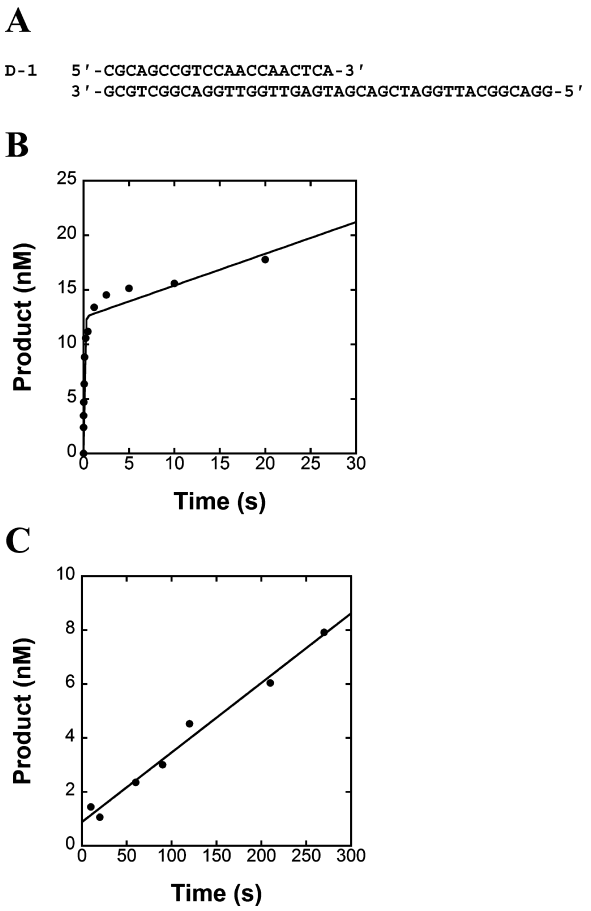

Figure 1. Pre-steady-state and steady-state kinetics of correct dTTP incorporation into a DNA substrate D-1 by Polε exo- at 20 °C. (A) The DNA substrate D-1 containing a 21-mer primer and a complementary 41-mer template. (B) A preincubated solution of Polε exo- (200 nM, UV concentration) and 5′-radiolabeled D-1 (120 nM) was rapidly mixed with dTTP (1.25 μM) and quenched at various time intervals with 0.37 M EDTA. The data were fit to eq 1 to yield a burst phase rate constant of 12 ± 2 s^{-1} and a linear phase rate constant of 0.023 ± 0.006 s^{-1}. (C) A preincubated solution of Polε exo- (1 nM, active site concentration) and 5′-radiolabeled D-1 (250 nM) was mixed with dTTP (100 μM) and quenched at various time intervals with 0.37 M EDTA. The data were fit to eq 2 to yield a steady-state rate constant of 0.026 s^{-1}.

A is the product concentration in the absence of the DNA trap, *k* is the DNA dissociation rate constant (k_{-1}), and *C* is the ^{32}P-labeled product concentration in the presence of a trap for unlimited time.

Active Site Titration Assay. The equilibrium dissociation constant (K_d^{DNA}) of the Polε exo-·DNA binary complex was determined by an active site titration. A preincubated solution of Polε exo- (64 nM, UV concentration) and increasing concentrations of 5′-radiolabeled D-1 DNA substrate (5−175 nM) was mixed rapidly with a solution containing dTTP (100 μM). Each time point was quenched at 50 ms to ensure

dx.doi.org/10.1021/bi400803v | *Biochemistry* 2013, 52, 7041−7049

maximum product formation. All reactions were repeated in triplicate. The products were quantified via sequencing gel analysis.

Processive Polymerization Assay. The processivity of Polε exo-, calculated as the average rate constant of nucleotide incorporation divided by the average rate constant of dissociation of the binary complex (E·DNA), was measured via a processive polymerization assay. A preincubated solution of Polε exo- (60 nM, active site concentration) and 5′-radiolabeled D-1 (100 nM) was rapidly mixed with a solution containing dTTP, dGTP, and dCTP (100 μM each). At various time points, the reaction was quenched with EDTA to a final concentration of 0.37 M. The products were separated by sequencing gel electrophoresis and quantified by computer simulation.

Elemental Effect of Nucleotide Incorporation. To measure the elemental effect of correct nucleotide incorporation, a preincubated solution of Polε exo- (40 nM, active site concentration) and 5′-radiolabeled D-1 (20 nM) was rapidly mixed with dTTP or S_p-dTTPαS (1.25 μM) in buffer E and quenched with 0.37 M EDTA at various time points. To measure the elemental effect of incorrect nucleotide incorporation, the same preincubated Polε exo- and D-1 solution was rapidly mixed with dATP or S_p-dATPαS (600 μM). The S_p isomers were used due to previously observed stereoselectivity.[15] All products were quantified by sequencing gel analysis.

Pulse-Chase and Pulse-Quench Experiments. To observe an enzyme conformational change preceding the chemistry step, a preincubated solution of Polε exo- (50 nM, active site concentration) and unlabeled D-1 (50 nM) was rapidly mixed with [α-^{32}P]dTTP (2.5 μM) for time points ranging from 4 to 650 ms. In the pulse-quench assay, reactions were quenched immediately with 1 M HCl. In the pulse-chase assay, reactions were chased with 1 mM unlabeled dTTP and were subsequently quenched with 1 M HCl after 30 s. For both the pulse-chase and the pulse-quench assays, acid-quenched mixtures were treated with chloroform and then neutralized in 1 M NaOH prior to analysis by PAGE.

Product Analysis. Reaction products were separated by denaturing PAGE (17% acrylamide, 8 M urea, and 1x TBE running buffer) and quantified by using a Typhoon TRIO (GE Healthcare) and ImageQuant (Molecular Dynamics). For product analysis of the pulse-chase and pulse-quench assays, reaction products were separated using a 20% highly cross-linked polyacrylamide gel matrix as described previously.[16]

Data Analysis. Data were fit by nonlinear regression using Kaleidagraph (Synergy Software).

Data from the burst assay were fit to eq 1

$$[\text{product}] = A[1 - \exp(-k_1 t) + k_2 t] \quad (1)$$

where A is the amplitude of active enzyme, k_1 is the observed burst rate constant, and k_2 is the observed steady-state rate constant.

Data from the experiments performed under steady-state conditions were fit to eq 2

$$[\text{product}] = k_{ss} E_0 t + E_0 \quad (2)$$

where k_{ss} is the steady-state rate constant of dNTP incorporation at the initial active enzyme concentration of E_0

For the active site titration experiment, the resulting product concentration (equivalent to burst amplitude) was plotted versus the concentration of D-1, and the data were fit to eq 3

$$[\text{E·DNA}] = 0.5(K_d^{\text{DNA}} + E_0 + D_0) - 0.5 [(K_d^{\text{DNA}} + E_0 + D_0)^2 - 4E_0D_0]^{1/2} \quad (3)$$

where K_d^{DNA} represents the equilibrium dissociation constant for the binary complex (E·DNA), E_0 is the active enzyme concentration, and D_0 is the DNA concentration.

Data from the experiments performed under single-turnover conditions were fit to eq 4

$$[\text{product}] = A[1 - \exp(-k_{obs} t)] \quad (4)$$

where A is the amplitude of product formation and k_{obs} is the observed single-turnover rate constant. The k_{obs} values were plotted against dTTP concentrations and the data were fit to eq 5

$$k_{obs} = k_p[\text{dTTP}]/(K_d^{\text{dTTP}} + [\text{dTTP}]) \quad (5)$$

where k_p is the maximum rate constant of dTTP incorporation and K_d^{dTTP} is the equilibrium dissociation constant of dTTP.

Data from the processive elongation of 21/41-mer to 27/41-mer were modeled by using KinTek Explorer (KinTek).[17]

RESULTS

Expression and Purification of an Exonuclease-Deficient Mutant of Human Polε. Because of the difficulty of preparing the four subunit Polε holoenzyme for pre-steady-state kinetic analysis, we chose to express and purify a 140 kDa N-terminal fragment of p261, the catalytic subunit of Polε, which has been characterized previously.[13] The truncation fragment spans from residues 1−1189 and contains all conserved polymerase and exonuclease motifs.[18] Previously, the polymerase function of this N-terminal fragment has been shown to be as active as that of the full-length catalytic subunit.[5] It is also known that the 140 kDa fragment possesses a very active 3′→5′ exonuclease function.[6] This exonuclease activity is expected to compete with the polymerization activity of the 140 kDa fragment and complicate the interpretation of kinetic data. To circumvent this issue, we prepared an exonuclease-deficient mutant of the 140 kDa fragment by substituting three highly conserved carboxylates D275, E277, and D368 with alanine (Figure 2). These residues are located within the Exo I and II sequence motifs, which are highly conserved among replicative, B-family DNA polymerases.[19] Substitution of these particular residues for alanine has resulted in successful generation of exonuclease-deficient B-family DNA polymerases.[10,20] The purified triple mutant of the 140-kDa fragment, denoted as

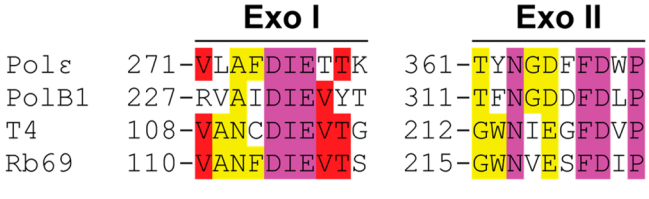

Figure 2. Conservation of Exo I and Exo II motifs across the B-family DNA polymerases. Exonuclease motifs I and II, marked by the sequences DxE and NxxxF, respectively, where x is any amino acid residue, are highly conserved in the B-family. Polε is DNA polymerase ε from human, PolB1 is DNA polymerase I from *Sulfolobus solfataricus*, T4 is DNA polymerase from bacteriophage T4, and Rb69 is DNA polymerase from bacteriophage Rb69. Absolutely conserved residues are shown in purple, highly conserved residues are in red, and semiconserved residues are in yellow.

dx.doi.org/10.1021/bi400803v | *Biochemistry* 2013, 52, 7041−7049

Polε exo-, was then tested for its polymerase and exonuclease activities. Polε exo- possessed the wild-type level of polymerase function but lacked any noticeable exonuclease activity even after an hour of its incubation with DNA and Mg^{2+} at 20 °C (data not shown). Thus, this triple mutant is suitable for pre-steady-state kinetic investigation of polymerization mechanism of Polε.

Burst Kinetics. Replicative DNA polymerases typically exhibit biphasic kinetics during single nucleotide incorporation.[9,10,21] A burst assay was used to observe whether Polε exo- also followed a similar biphasic pattern. Specifically, a preincubated solution of Polε exo- (200 nM, UV concentration) and 5′-radiolabeled DNA substrate D-1 (120 nM, Figure 1A) was rapidly mixed with correct dTTP (1.25 μM) in buffer E (see Experimental Procedures) for various times at 20 °C. Notably, 37 °C was not used because the rate constant of product formation catalyzed by Polε exo- (k_p > 500 s^{-1}) was too fast to be accurately measured by using a rapid chemical quench apparatus. The time course for product formation reveals biphasic kinetics characterized by a burst of product formation followed by a slower linear phase (Figure 1B). This suggests that Polε exo-, as other kinetically characterized DNA polymerases,[9,10,21−23] likely follows the same minimal kinetic mechanism (Scheme 1) when catalyzing correct nucleotide incorporation.[24] The burst rate constant of nucleotide incorporation was determined to be 12 ± 2 s^{-1} while the linear phase occurred with a rate constant of 0.023 ± 0.006 s^{-1} (Figure 1B). To evaluate if the linear phase rate constant was the steady-state rate constant of nucleotide incorporation, we measured the steady-state rate constant directly. Polε exo- (1 nM, active site concentration) was preincubated with a large excess of D-1 (250 nM) and then mixed with dTTP (100 μM) for various time intervals. The observed steady-state rate constant was 0.026 s^{-1} (Figure 1C), which is nearly identical to the rate constant of the linear phase in Figure 1B, suggesting that the linear phase was indeed the steady-state phase of product formation. The steady-state rate of polymerase-catalyzed nucleotide incorporation is usually representative of the slow dissociation rate of the E·DNA binary complex, which limits the rate of multiple turnovers.[10] To confirm that Polε exo- exhibited the same pattern, we directly measured the rate of DNA dissociation. A preincubated solution of Polε exo- (50 nM) and D-1 (100 nM) was mixed with unlabeled trap D-1 (2.5 μM) for various times. Then dTTP (133 μM) was added for 15 s to allow extension of any labeled D-1 bound by Polε exo- (E·DNA). The data were fit to a single-exponential equation (see Experimental Procedures) to yield an E·DNA dissociation rate constant (k_{-1}) of 0.021 ± 0.007 s^{-1} (Figure 3 and Table 1), which is similar to the measured steady-state rate constant of 0.023 ± 0.006 s^{-1}. Thus, we conclude that the aforementioned steady-state or linear phase (Figure 1) was limited by DNA dissociation from the E·DNA binary complex.

Active Site Titration. The burst phase in Figure 1B suggests the formation of a stable binary complex (E·DNA) which bound and incorporated dTTP rapidly during the first turnover. Thus, the equilibrium dissociation constant (K_d^{DNA}) of the binary complex can be measured by titrating the active site of Polε exo- with varying concentrations of DNA based on the fact that the amount of E·DNA complex formed is given by the amplitude of the first turnover.[21] A preincubated solution of Polε exo- (64 nM, UV concentration) and increasing concentrations of 5′-radiolabeled D-1 (5−175 nM) was rapidly mixed with dTTP (100 μM) and Mg^{2+} for 50 ms, allowing ample time for full product formation before being quenched by EDTA. Each reaction was repeated in triplicate, and the mean product concentration (E·DNA) was plotted versus the DNA concentration. The data were then fit to a quadratic equation (eq 3) to yield a K_d^{DNA} of 79 ± 14 nM (Table 1) and an active enzyme concentration (E_0) of 10.1 ± 0.9 nM (Figure 4). Based on the UV concentration, only 15.8% of Polε exo- was active although the protein was purified to greater than 95% homogeneity based on the result of SDS-PAGE (data not shown). Henceforth, all experiments described below were performed using the active site concentration of Polε exo-. From the above measured E·DNA dissociation rate constant (k_{-1}) of 0.021 s^{-1}, the second-order rate constant of DNA

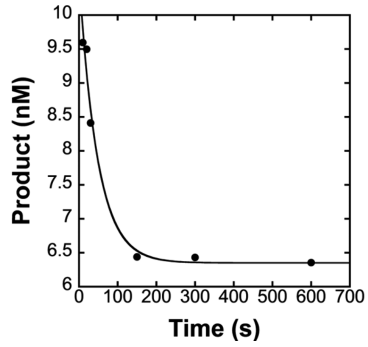

Figure 3. DNA dissociation from the Polε·D-1 binary complex. A preincubated solution of Polε exo- (50 nM) and 5′-radiolabeled D-1 (100 nM) was mixed with an unlabeled D-1 trap (2.5 μM) for various times. Then dTTP (133 μM) was added for 15 s before quenching with 0.37 M EDTA. The data were fit to the equation [product] = A exp(−kt) + C to yield a dissociation rate constant (k_{-1}) of 0.021 ± 0.007 s^{-1}.

Table 1. Kinetic Parameters for Correct Nucleotide Incorporation Catalyzed by Polε exo- at 20 °C

parameter	value	parameter	value
k_1	0.27 μM^{-1} s^{-1}	k_{-2}	3100 s^{-1}
k_{-1}	0.021 s^{-1}	K_d^{dTTP}	31 μM
K_d^{DNA}	79 nM	k_3	248 s^{-1}
k_2	100 μM^{-1} s^{-1}	k_7	5 s^{-1}

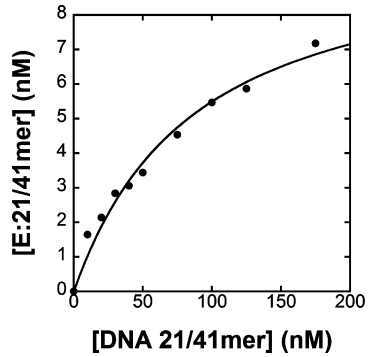

Figure 4. Active site titration of Polε exo- at 20 °C. A preincubated solution of Polε exo- (64 nM, UV concentration) and increasing concentrations of 5′-radiolabeled D-1 (5−175 nM) was rapidly mixed with dTTP (100 μM). All reactions were quenched after 50 ms with 0.37 M EDTA. The product concentrations were plotted versus D-1 concentrations, and the data were fit to eq 3, yielding a K_d^{DNA} of 79 ± 14 nM for the equilibrium dissociation constant of the Polε exo-·D-1 complex and an enzyme amplitude of 10.1 ± 0.9 nM.

dx.doi.org/10.1021/bi400803v | Biochemistry 2013, 52, 7041−7049

binding ($k_1 = k_{-1}/K_d^{DNA}$) was calculated to be 2.7×10^5 M^{-1} s^{-1} (Table 1).

Pre-Steady-State Kinetics of Correct dTTP Incorporation by Polε exo-. Following the DNA binding event, Polε exo- binds an incoming nucleotide to form the ground-state E·DNA·dNTP ternary complex. To the measure both the maximum rate constant of correct nucleotide incorporation (k_p) catalyzed by Polε exo- as well as the equilibrium dissociation constant (K_d^{dTTP}) for a correct incoming nucleotide, we carried out a series of single-turnover experiments with increasing concentrations of correct dTTP. A preincubated solution of Polε exo- (80 nM) and 5′-radiolabeled D-1 (20 nM) was mixed rapidly with dTTP (0.625−200 μM) for various times. For each dTTP concentration, the product concentration was plotted against reaction time, and the data were fit to a single-exponential equation (eq 4) to yield k_{obs} (Figure 5A). The k_{obs} values were then plotted against the corresponding dTTP concentrations, and the data were fit to a hyperbolic equation (eq 5) to yield a k_p of 248 ± 6 s^{-1} (k_3) and a K_d^{dTTP} of 31 ± 2 μM (Table 1 and Figure 5B). Furthermore, if the association rate constant (k_2) of a small molecule dTTP approaches the diffusion limit of 1.0×10^8 M^{-1} s^{-1}, the upper limit of the dTTP dissociation rate constant ($k_{-2} = k_2 K_d^{dTTP}$) was calculated to be 3100 s^{-1} (Table 1), which is too fast to be measured by current pre-steady-state techniques.

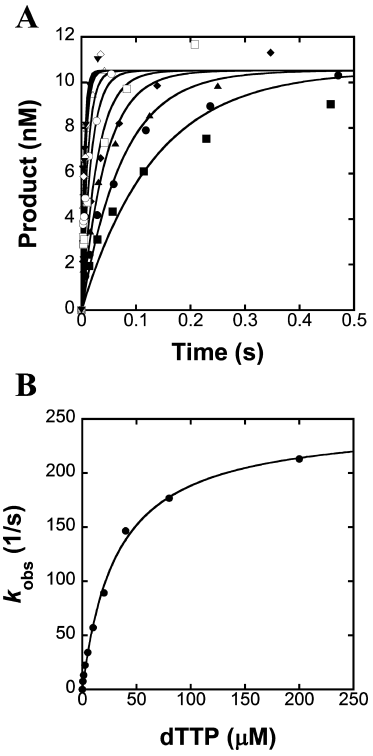

Figure 5. Concentration dependence on the pre-steady-state rate constant of correct dTTP incorporation catalyzed by Polε exo- at 20 °C. (A) A preincubated solution of Polε exo- (80 nM) and 5′-radiolabeled D-1 (20 nM) was mixed with increasing concentrations of dTTP [0.625 (■), 1.25 (●), 2.5 (▲), 5 (♦), 10 (□), 20 (○), 40 (△), 80 (◊), and 200 μM (▼)] for various times. The solid lines are the best fits to eq 4. (B) The observed rate constants of product formation (k_{obs}) were plotted versus dTTP concentrations. The data were then fit to eq 5 to yield a k_p of 248 ± 6 s^{-1} and a K_d^{dTTP} of 31 ± 2 μM.

Processive Polymerization. The processivity of a DNA polymerase is defined as the number of nucleotides incorporated by the polymerase per DNA binding event, which can be quantitatively estimated as the ratio of the polymerization rate constant divided by the DNA dissociation rate constant. To kinetically measure this ratio, a preincubated solution of Polε exo- (60 nM) and 5′-radiolabeled D-1 (100 nM) was mixed with three nucleotides (100 μM each) for various times to allow the primer 21-mer to be elongated into a 27-mer product. The DNA substrate was used in molar excess over Polε exo-, which was to ensure that the measured kinetics of sequential elongation steps were a function of single enzyme binding events. The time courses of D-1 and products (Figure 6) were fit to a mechanism consisting of six consecutive nucleotide incorporation and dissociation events by the computer simulation program KinTek Explorer.[17] The rate constants of each intermediate product formation was 169 ± 6 s^{-1} for 22-mer, 20 ± 1 s^{-1} for 23-mer, 14 ± 1 s^{-1} for 24-mer, 79 ± 20 s^{-1} for 25-mer, 30 ± 5 s^{-1} for 26-mer, and 36 ± 4 s^{-1} for 27-mer. Thus, the rate constant of polymerization is in the range of 14−169 s^{-1} with an average of 58 s^{-1}. The following DNA dissociation rate constants were also generated: 12 ± 1 s^{-1} for 22/41-mer, 2.2 ± 0.9 s^{-1} for 23/41-mer, 6.2 ± 4.0 s^{-1}

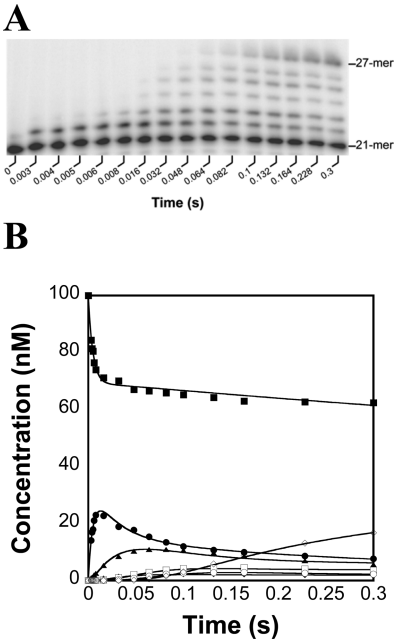

Figure 6. Processive polymerization catalyzed by Polε exo- at 20 °C. A preincubated solution of Polε exo- (60 nM) and 5′-radiolabeled D-1 (100 nM) was rapidly mixed with dTTP, dCTP, and dGTP (100 μM) for various time intervals before being quenched by 0.37 M EDTA. Products were resolved by sequencing gel electrophoresis. (A) Gel image of the processivity assay. (B) The amount of remaining substrate [21-mer (■)] and each intermediate product [22-mer (●), 23-mer (▲), 24-mer (♦), 25-mer (□), 26-mer (○), and 27-mer (◇)] were plotted as a function of time. The solid lines represent the best fits generated by computer simulation using a model consisting of six single nucleotide incorporation events and six DNA dissociation events. The polymerization rate constants were 169 ± 6 s^{-1} for 22-mer, 20 ± 1 s^{-1} for 23-mer, 14 ± 1 s^{-1} for 24-mer, 79 ± 20 s^{-1} for 25-mer, 30 ± 5 s^{-1} for 26-mer, and 36 ± 4 s^{-1} for 27-mer. The dissociation rate constants were 12 ± 1 s^{-1} for 22/41-mer, 2.2 ± 0.9 s^{-1} for 23/41-mer, 6.2 ± 4.0 s^{-1} for 24/41-mer, 4.0 ± 1.9 s^{-1} for 25/41-mer, 2.2 ± 1.1 s^{-1} for 26/41-mer, and 0.9 ± 0.2 s^{-1} for 27/41-mer.

dx.doi.org/10.1021/bi400803v | Biochemistry 2013, 52, 7041−7049

for 24/41-mer, 4.0 ± 1.9 s^{-1} for 25/41-mer, 2.2 ± 1.1 s^{-1} for 26/41-mer, and 0.9 ± 0.2 s^{-1} for 27/41-mer. These DNA dissociation rate constants (0.9−12 s^{-1}) are significantly larger than the above-measured E·DNA dissociation rate constant (0.021−0.026 s^{-1}) and reflected the rates for the dissociation of various E·DNA·dNTP complexes during processive polymerization.[10] Similar fast DNA dissociation rates were also observed for other replicative polymerases such as *S. solfataricus* PolB1, *Staphylococcus aureus* PolC, T4 DNA polymerase, and HIV-1 RT.[9,10,25,26] Based on the average rate constants of polymerization (58 s^{-1}) and E·DNA·dNTP dissociation (5 s^{-1}, Table 1, k_7), the processivity of Polε exo- was calculated to be 11.

Elemental Effect of Nucleotide Incorporation. The observation of a distinct burst phase in Figure 1B suggests that a single nucleotide incorporation cycle is limited by either phosphodiester bond formation (step 4 in Scheme 1), a conformational change preceding phosphodiester bond formation (step 3 in Scheme 1), or both. To probe the rate-limiting step, single-turnover measurements were carried out with both dTTP and S_p-dTTPαS. S_p-dTTPαS contains a nonbridging phosphothioate substitution at the α-phosphate where bond breakage and formation take place. A preincubated solution of Polε exo- (40 nM) and 5′-radiolabeled D-1 (20 nM) was rapidly mixed with dTTP or S_p-dTTPαS (1.25 μM). Data were fit to a single-exponential equation (eq 4) to give k_{obs} values of 9 ± 1 and 10 ± 1 s^{-1} for the incorporation of dTTP and S_p-dTTPαS, respectively (Figure 7A). An elemental effect of 0.9 for correct incorporation of dTTP was calculated from these k_{obs} values. Previously, an elemental effect of 4−11 has been used as a suggestive evidence for a rate-limiting chemistry step.[27] Thus, our result suggests that the rate of correct nucleotide incorporation catalyzed by Polε exo- is probably not limited by step 4 in Scheme 1.

To determine whether step 3 or 4 in Scheme 1 was rate-limiting for incorrect nucleotide incorporation, k_{obs} was measured for the incorporation of incorrect dATP or its analogue S_p-dATPαS (600 μM) into D-1. The k_{obs} values were determined to be 0.25 ± 0.02 and 0.0015 s^{-1} for the incorporation of dATP and S_p-dATPαS, respectively, giving an elemental effect of 167 (Figure 7B). This large elemental effect suggests that the chemistry step during incorrect nucleotide incorporation catalyzed by Polε exo- is likely rate-limiting.[27] Similar elemental effect values for correct and incorrect nucleotide incorporations have previously been obtained for *S. solfataricus* PolB1.[10] However, a large elemental effect may be due to steric clash between active site residues and the polymerase-bound nucleotide caused by the sulfur atom substitution.[24] Thus, more evidence is required to identify the rate-limiting step for correct or incorrect nucleotide incorporation catalyzed by Polε exo-.

Pulse-Chase and Pulse-Quench Experiments. To provide more conclusive evidence for diagnosing the rate-limiting step, we performed pulse-chase and pulse-quench assays which have been used to identify the rate-liming protein conformational change (step 3 in Scheme 1) for other DNA polymerases.[10,23,24,28] If the conformational change step also exists with Polε exo-, we would expect to see an increase in product formation for the pulse-chase assay relative to the pulse-quench assay. A preincubated solution of Polε exo- (50 nM) and unlabeled D-1 (50 nM) was mixed rapidly with [α-^{32}P]dTTP (2.5 μM) for various times. In the pulse-chase assay, each reaction was chased with a large excess of unlabeled

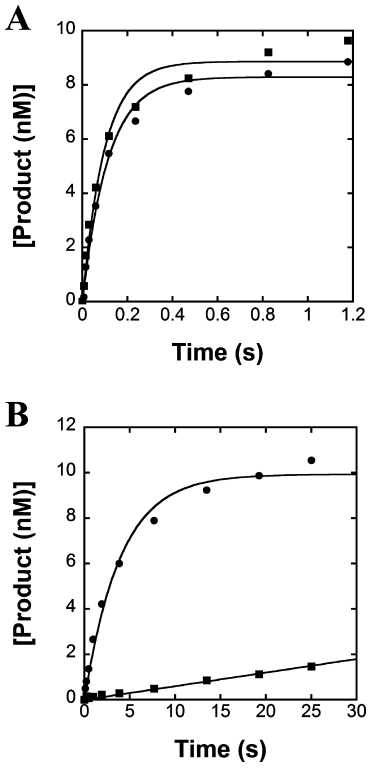

Figure 7. Elemental effect on the rate constant of correct and incorrect nucleotide incorporation catalyzed by Polε exo- at 20 °C. (A) A preincubated solution of Polε exo- (40 nM) and 5′-radiolabeled D-1 (20 nM) was rapidly mixed with 1.25 μM dTTP (●) or S_p-dTTPαS (■) in parallel time courses. The data were fit to eq 4 to yield k_{obs} values of 9 ± 1 and 10 ± 1 s^{-1} for dTTP and S_p-dTTPαS, respectively. The elemental effect was calculated to be 0.9. (B) The same Polε exo- and D-1 solution was rapidly mixed with 600 μM dATP (●) or S_p-dATP (■) in parallel time courses. The data were fit to eq 4 for dATP and a linear fit for S_p-dATPαS. The k_{obs} values were 0.25 ± 0.02 and 0.0015 s^{-1} for dATP and S_p-dATPαS, respectively. The elemental effect was calculated to be 167.

dTTP (1 mM) for an additional 30 s before being quenched with 1 M HCl. In the pulse-quench assay, the reactions were quenched immediately with 1 M HCl without the addition of unlabeled dTTP.

During each pulse-chase assay, the E·DNA·dNTP complex that was in equilibrium with the forward and reverse intermediate species would presumably be pushed in the forward direction by the chase with a large molar excess of unlabeled dTTP, thus increasing product formation. This result would suggest that the chemistry step is preceded by a stable E·DNA·dNTP ternary complex that is distinct from the ground-state ternary complex. A product formation rate constant of 69 ± 8 s^{-1} and amplitude of 21.7 ± 0.7 nM were determined for the pulse-chase assay, whereas they were 66 ± 6 s^{-1} and 15.3 ± 0.5 nM for the pulse-quench assay (Figure 8). Since the reactions in the two sets of assays are the same, the incorporation rates were expected to be equal, and this condition was met based on almost identical measured product formation rates. In contrast, the amplitude difference of 6.4 nM (42%) suggests the existence of a stable and distinct complex that accumulated prior to the chemistry step and was chased into the product by large molar excess of cold dTTP. The stable intermediate could be E·DNA, E·DNA·dNTP, or E′·DNA·dNTP in Scheme 1. However, it was not the E·DNA binary

dx.doi.org/10.1021/bi400803v | *Biochemistry* 2013, 52, 7041−7049

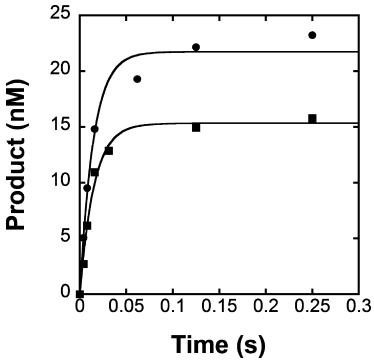

Figure 8. Pulse-chase and pulse-quench experiments at 20 °C. A preincubated solution of Polε exo- (50 nM) and unlabeled D-1 (50 nM) was rapidly mixed [α-^{32}P]dTTP (2.5 μM) for various time intervals. The pulse-quench (■) reaction mixtures were immediately quenched with 1 M HCl while the pulse-chase (●) reaction mixtures were chased with an excess of unlabeled dTTP (1 mM) for 30 s, followed by acid-quenching. The data were fit to eq 4 to yield a reaction rate constant of 69 ± 8 s^{-1} and a reaction amplitude of 21.7 ± 0.7 nM for the pulse-chase assay and 66 ± 6 s^{-1} and 15.3 ± 0.5 nM for the pulse-quench assay.

complex since it would bind cold dTTP under the pulse-chase conditions, form undetectable cold product, and lead to no change in reaction amplitude between the pulse-chase and pulse-quench assays. Similarly, the stable intermediate was not the E·DNA·dNTP complex either since the 42% amplitude difference would require that the complex partitioned between product formation (58%, 66 s^{-1}), dTTP dissociation to form the E·DNA binary complex (calculated as [66/(58%) − 66 − 5] = 43 s^{-1} based on the kinetic partitioning from E·DNA·dNTP to E·product, E·DNA, and E + DNA + dNTP), and the dissociation of E·DNA·dNTP to form E, DNA, and dNTP (average rate constant = 5 s^{-1}, Scheme 1, k_7). In comparison, the rate constant for the E·DNA·dNTP dissociation (k_{-2} in Scheme 1) to form the E·DNA complex has been estimated to be 3100 s^{-1} (Table 1), which is much larger than 43 s^{-1}. Thus, the stable complex had to be E′·DNA·dNTP, not E·DNA·dNTP. Alternatively, this conclusion can be reached based on the facts that the formation of E·DNA·dNTP from E·DNA and dNTP was a rapid equilibrium and k_{-2} (3100 s^{-1}) in Scheme 1 was much faster than the product or the stable intermediate formation rate constant (66–69 s^{-1}) as measured in Figure 8. Lastly, in order for E′·DNA·dNTP (21.7 − 15.3 = 6.4 nM) to accumulate, a slow conformational change step (step 5 in Scheme 1) after the rapid chemistry step must occur and serve as a kinetic "roadblock".[22] This step resulted in 15.3 nM of E′·DNA_{n+1}·PPi (Scheme 1) and a calculated internal equilibrium constant of 2.4 (= 15.3/6.4).[22]

■ DISCUSSION

In this paper, we carried out pre-steady-state kinetic studies in order to establish a minimal kinetic mechanism for correct nucleotide incorporation catalyzed by Polε exo-, an N-terminal truncation fragment of the catalytic subunit of human Polε. The burst assay revealed that correct dTTP incorporation exhibited biphasic kinetics characterized by a "burst" phase for the first turnover followed by a slow linear phase (Figure 1B). The latter phase was demonstrated to represent the steady-state phase of product formation during subsequent turnovers (Figure 1C). A DNA trap assay further confirmed that the steady-state phase was limited by the E·DNA dissociation. These kinetic assays suggest that Polε exo- catalyzes correct nucleotide incorporation by following a similar mechanism (Scheme 1) which has been established for numerous DNA polymerases and reverse transcriptases.[24] With this mechanism, Polε exo- first binds a DNA substrate to form the E·DNA binary complex and then an incoming nucleotide to form the E·DNA·dNTP ground-state ternary complex. Through the active site titration assay, the observed equilibrium dissociation constant K_d^{DNA} for the formation of E·DNA from Polε exo- and the DNA substrate D-1 (Figure 1A) was determined to be 79 nM (Figure 4). The K_d^{dTTP} for correct dTTP binding to E·DNA was then measured to be 31 μM (Figure 5B). To identify the rate-limiting step for single nucleotide incorporation during the first turnover, two lines of kinetic evidence were provided. First, a small elemental effect of 0.9 was determined for the incorporation of correct dTTP versus its thio-analogue S_p-dTTPαS (Figure 7A), suggesting that the chemistry step was unlikely rate-limiting since the elemental effect fell significantly outside the elemental effect range of 4–11 for a rate-limiting chemical reaction.[27] In contrast, a much larger elemental effect (167) was determined for incorrect dNTP incorporation (Figure 7B). These elemental effect values suggest that correct and incorrect nucleotide incorporations did not share the same rate-limiting step and that the chemistry step (step 4 in Scheme 1) at least partially controlled the rate of incorrect nucleotide incorporation. However, as noted previously, elemental effect measurements alone are not substantial pieces of evidence for the absence or presence of a rate-limiting conformational change preceding chemistry because an unusually large elemental effect or an elemental effect just below the expected range of 4–11 is difficult to interpret and the elemental effect is significantly affected by the exact active site structure of E′·DNA·dNTP.[15,24] To provide more definitive evidence for the rate-limiting step for correct dTTP incorporation, we performed pulse-chase and pulse-quench assays. There was a 42% reaction amplitude difference (Figure 8) between the pulse-chase and pulse-quench assays, which suggested that a stable intermediate complex E′·DNA·dNTP accumulated prior to step 4 in Scheme 1. The observed accumulation of E′·DNA·dNTP further indicates the presence of two slow steps (steps 3 and 5) that flank the fast chemistry step (step 4) in Scheme 1.[22,23] Thus, step 3 limited dTTP incorporation in the forward direction while step 5 controlled the reverse polymerization direction or pyrophosphorolysis and served as a kinetic "roadblock" (Scheme 1).

The processivity of Polε exo- was estimated to be 11 nucleotide incorporations per DNA binding event at 20 °C, given by the ratio of the average polymerization rate constant (58 s^{-1}) divided by the average E·DNA·dNTP dissociation rate constant (5 s^{-1}). The calculated processivity of Polε exo- is remarkably lower than that of other replicative DNA polymerases[21,29] and is inadequate for catalyzing leading-strand synthesis *in vivo*. However, the pre-steady-state rates used for calculating the processivity values for T7 DNA polymerase and human mitochondrial DNA polymerase were measured in the presence of their processivity cofactors. For example, *E. coli* thioredoxin, the cofactor of T7 DNA polymerase, has been shown to increase the processivity of this replicative enzyme by more than 2 orders of magnitude.[30] The low processivity of Polε exo- is mainly contributed by the high dissociation rate constant measured in the absence of any cofactors. Previously, proliferating cell nuclear antigen (PCNA) has been shown to enhance DNA synthesis catalyzed by Polε.[5] Similarly, PCNA

has also been demonstrated to significantly enhance the processivity of mammalian Polδ.[31,32] Taken together, PCNA is likely to be the processivity cofactor for Polε during leading-strand synthesis, and we are currently investigating this possibility.

Notably, the measured K_d^{DNA} (79 nM) of Polε exo- (Figure 4) is roughly 4−40-fold higher than those of DNA polymerases from the A-, B-, and Y-families.[10,21−23,25] The low DNA binding affinity of Polε exo- could be caused by the absence of the smaller subunits of the Polε holoenzyme. *Saccharomyces cerevisiae* Dpb3p and Dpb4p, which are respectively homologous to the p12 and p17 subunits of the Polε holoenzyme, contain a double-stranded DNA binding site.[33] Thus, it is possible that the presence of p12 and p17 will enhance the DNA binding affinity of Polε. In addition, PCNA, which has been shown to stimulate Polε activity *in vitro*,[34] may also improve the DNA binding affinity of Polε. Similar conclusions have been drawn for T4 DNA polymerase, which possesses a comparable K_d^{DNA} of 70 nM in the absence of any replication factors,[9] and yeast Polδ, which binds DNA with a 5-fold tighter affinity in the presence than in the absence of PCNA.[35]

In summary, our kinetic analysis demonstrates that Polε exo-, like other replicative DNA polymerases, extends DNA via an induced-fit mechanism. The studies presented here will provide a foundation for future kinetic investigation of human Polε holoenzyme.

AUTHOR INFORMATION

Corresponding Author

*Tel (614) 688-3706; Fax (614) 292-6773; e-mail suo.3@osu.edu (Z.S.).

Funding

This work was supported by National Institutes of Health grant (GM079403) and National Science Foundation grant (MCB-0960961) to Z.S. and an REU training grant (DBI-1062144) to S.K.

Notes

The authors declare no competing financial interest.

ABBREVIATIONS

Polα, DNA polymerase α; Polδ, DNA polymerase δ; Polε, DNA polymerase ε; PolB1, *Sulfolobus solfataricus* P2 DNA polymerase B1; dNTP, 3′-deoxynucleotide 5′-triphosphate; GST, glutathione S-transferase; TEV, tobacco etch virus; IPTG, isopropyl β-D-1-thiogalactopyranoside; EDTA, ethylenediaminetetraacetic acid; DTT, dithiothreitol; BSA, bovine serum albumin; PCNA, proliferating cell nuclear antigen; PAGE, polyacrylamide gel electrophoresis; HIV-1 RT, human immunodeficiency virus type 1 reverse transcriptase.

REFERENCES

(1) Kunkel, T. A., and Burgers, P. M. (2008) Dividing the workload at a eukaryotic replication fork. *Trends Cell Biol. 18*, 521−527.

(2) Waga, S., and Stillman, B. (1994) Anatomy of a DNA replication fork revealed by reconstitution of SV40 DNA replication in vitro. *Nature 369*, 207−212.

(3) McElhinny, S. A. N., Gordenin, D. A., Stith, C. M., Burgers, P. M. J., and Kunkel, T. A. (2008) Division of labor at the eukaryotic replication fork. *Mol. Cell 30*, 137−144.

(4) Pursell, Z. F., Isoz, I., Lundstrom, E. B., Johansson, E., and Kunkel, T. A. (2007) Yeast DNA polymerase epsilon participates in leading-strand DNA replication. *Science 317*, 127−130.

(5) Bermudez, V. P., Farina, A., Raghavan, V., Tappin, I., and Hurwitz, J. (2011) Studies on human DNA polymerase epsilon and GINS complex and their role in DNA replication. *J. Biol. Chem. 286*, 28963−28977.

(6) Hamatake, R. K., Hasegawa, H., Clark, A. B., Bebenek, K., Kunkel, T. A., and Sugino, A. (1990) Purification and characterization of DNA polymerase II from the yeast Saccharomyces cerevisiae. Identification of the catalytic core and a possible holoenzyme form of the enzyme. *J. Biol. Chem. 265*, 4072−4083.

(7) Kunkel, T. A. (2004) DNA replication fidelity. *J. Biol. Chem. 279*, 16895−16898.

(8) Parlanti, E., Locatelli, G., Maga, G., and Dogliotti, E. (2007) Human base excision repair complex is physically associated to DNA replication and cell cycle regulatory proteins. *Nucleic Acids Res. 35*, 1569−1577.

(9) Capson, T. L., Peliska, J. A., Kaboord, B. F., Frey, M. W., Lively, C., Dahlberg, M., and Benkovic, S. J. (1992) Kinetic characterization of the polymerase and exonuclease activities of the gene 43 protein of bacteriophage T4. *Biochemistry 31*, 10984−10994.

(10) Brown, J. A., and Suo, Z. (2009) Elucidating the kinetic mechanism of DNA polymerization catalyzed by Sulfolobus solfataricus P2 DNA polymerase B1. *Biochemistry 48*, 7502−7511.

(11) Dieckman, L. M., Johnson, R. E., Prakash, S., and Washington, M. T. (2010) Pre-steady state kinetic studies of the fidelity of nucleotide incorporation by yeast DNA polymerase delta. *Biochemistry 49*, 7344−7350.

(12) Fiala, K. A., and Suo, Z. (2004) Pre-steady-state kinetic studies of the fidelity of Sulfolobus solfataricus P2 DNA polymerase IV. *Biochemistry 43*, 2106−2115.

(13) Korona, D. A., Lecompte, K. G., and Pursell, Z. F. (2010) The high fidelity and unique error signature of human DNA polymerase epsilon. *Nucleic Acids Res. 39*, 1763−1773.

(14) Hsieh, J. C., Zinnen, S., and Modrich, P. (1993) Kinetic mechanism of the DNA-dependent DNA polymerase activity of human immunodeficiency virus reverse transcriptase. *J. Biol. Chem. 268*, 24607−24613.

(15) Liu, J., and Tsai, M. D. (2001) DNA polymerase beta: pre-steady-state kinetic analyses of dATP alpha S stereoselectivity and alteration of the stereoselectivity by various metal ions and by site-directed mutagenesis. *Biochemistry 40*, 9014−9022.

(16) Arnold, J. J., Ghosh, S. K., and Cameron, C. E. (1999) Poliovirus RNA-dependent RNA polymerase (3D(pol)). Divalent cation modulation of primer, template, and nucleotide selection. *J. Biol. Chem. 274*, 37060−37069.

(17) Johnson, K. A. (2009) Fitting enzyme kinetic data with KinTek Global Kinetic Explorer. *Methods Enzymol. 467*, 601−626.

(18) Pursell, Z. F., Isoz, I., Lundstrom, E. B., Johansson, E., and Kunkel, T. A. (2007) Regulation of B family DNA polymerase fidelity by a conserved active site residue: characterization of M644W, M644L and M644F mutants of yeast DNA polymerase epsilon. *Nucleic Acids Res. 35*, 3076−3086.

(19) Iwai, T., Kurosawa, N., Itoh, Y. H., Kimura, N., and Horiuchi, T. (2000) Sequence analysis of three family B DNA polymerases from the thermoacidophilic crenarchaeon Sulfurisphaera ohwakuensis. *DNA Res. 7*, 243−251.

(20) Frey, M. W., Nossal, N. G., Capson, T. L., and Benkovic, S. J. (1993) Construction and characterization of a bacteriophage T4 DNA polymerase deficient in 3′−>5′ exonuclease activity. *Proc. Natl. Acad. Sci. U. S. A. 90*, 2579−2583.

(21) Patel, S. S., Wong, I., and Johnson, K. A. (1991) Pre-steady-state kinetic analysis of processive DNA replication including complete characterization of an exonuclease-deficient mutant. *Biochemistry 30*, 511−525.

(22) Dahlberg, M. E., and Benkovic, S. J. (1991) Kinetic mechanism of DNA polymerase I (Klenow fragment): identification of a second conformational change and evaluation of the internal equilibrium constant. *Biochemistry 30*, 4835−4843.

(23) Fiala, K. A., and Suo, Z. (2004) Mechanism of DNA polymerization catalyzed by Sulfolobus solfataricus P2 DNA polymerase IV. *Biochemistry 43*, 2116−2125.
(24) Joyce, C. M., and Benkovic, S. J. (2004) DNA polymerase fidelity: kinetics, structure, and checkpoints. *Biochemistry 43*, 14317−14324.
(25) Kati, W. M., Johnson, K. A., Jerva, L. F., and Anderson, K. S. (1992) Mechanism and fidelity of HIV reverse transcriptase. *J. Biol. Chem. 267*, 25988−25997.
(26) Lahiri, I., Mukherjee, P., and Pata, J. D. (2013) Kinetic characterization of exonuclease-deficient Staphylococcus aureus PolC, a C-family replicative DNA polymerase. *PLoS One 8*, e63489.
(27) Herschlag, D., Piccirilli, J. A., and Cech, T. R. (1991) Ribozyme-catalyzed and nonenzymatic reactions of phosphate diesters: rate effects upon substitution of sulfur for a nonbridging phosphoryl oxygen atom. *Biochemistry 30*, 4844−4854.
(28) Fiala, K. A., Sherrer, S. M., Brown, J. A., and Suo, Z. (2008) Mechanistic consequences of temperature on DNA polymerization catalyzed by a Y-family DNA polymerase. *Nucleic Acids Res. 36*, 1990−2001.
(29) Johnson, A. A., and Johnson, K. A. (2001) Fidelity of nucleotide incorporation by human mitochondrial DNA polymerase. *J. Biol. Chem. 276*, 38090−38096.
(30) Tabor, S., Huber, H. E., and Richardson, C. C. (1987) Escherichia coli thioredoxin confers processivity on the DNA polymerase activity of the gene 5 protein of bacteriophage T7. *J. Biol. Chem. 262*, 16212−16223.
(31) Prelich, G., Kostura, M., Marshak, D. R., Mathews, M. B., and Stillman, B. (1987) The cell-cycle regulated proliferating cell nuclear antigen is required for SV40 DNA replication in vitro. *Nature 326*, 471−475.
(32) Tan, C. K., Castillo, C., So, A. G., and Downey, K. M. (1986) An auxiliary protein for DNA polymerase-delta from fetal calf thymus. *J. Biol. Chem. 261*, 12310−12316.
(33) Tsubota, T., Maki, S., Kubota, H., Sugino, A., and Maki, H. (2003) Double-stranded DNA binding properties of Saccharomyces cerevisiae DNA polymerase epsilon and of the Dpb3p-Dpb4p subassembly. *Genes Cells 8*, 873−888.
(34) Chilkova, O., Stenlund, P., Isoz, I., Stith, C. M., Grabowski, P., Lundstrom, E. B., Burgers, P. M., and Johansson, E. (2007) The eukaryotic leading and lagging strand DNA polymerases are loaded onto primer-ends via separate mechanisms but have comparable processivity in the presence of PCNA. *Nucleic Acids Res. 35*, 6588−6597.
(35) Einolf, H. J., and Guengerich, F. P. (2000) Kinetic analysis of nucleotide incorporation by mammalian DNA polymerase delta. *J. Biol. Chem. 275*, 16316−16322.